International Journal of Smart Home
Vol. 10, No. 3, (2016), pp.271-284
http://dx.doi.org/10.14257/ijsh.2016.10.3.26

NLOS Channel Identification Based on Energy Detector for 60 GHz Wireless Communication Systems

Xiao-Lin Liang[1], Hao Zhang[1,2], Ting-Ting Lu[1] and T. Aaron. Gulliver[2]

[1]College of Information Science and Engineering, Ocean University of China, Qingdao, 266100, China
[2]Department of Electrical and Computer Engineering, University of Victoria, Victoria V8W 3P6, Canada
[1]xiaolin87liang@163.com, [2]zhanghao@ouc.edu.cn,
[3]lvtingting33@163.com, [4]agullive@ece.uvic.ca

Abstract

The major problem of indoor localization is presence of Non-line-of-sight (NLOS) channels. In order to perform NLOS identification, in this paper, we propose a novel NLOS identification technique based on threshold selection using the ratio of kurtosis and maximum slope of energy block of the received signal using energy detector. In particular, IEEE 802.15.3c 60 GHz channel models are used as examples and above statistics is found to be explained in detail. The simplicity of the proposed approach lies in use of parameters of energy-based time of arrival (TOA) estimation algorithm. The CM1 (LOS) and CM2 (NLOS) of IEEE 802.15.3c channel models are used. Numerical simulated results show that the correct identification of channel models with the proposed approach is better than with the multipath channel statistics based approach.

Keywords: *NLOS identification, kurtosis, maximum slope, 60 GHz, energy detector, IEEE 802.15.3c*

1. Introduction

The location of a mobile terminal (MT) can be estimated using different parameters of a received signal, such as TOA, angle-of-arrival (AOA), and/or the received signal strength (RSS). Impulse radio-60 GHz has a great potential for accurate ranging and localization systems due to its very wide bandwidth and capability in resolving individual multipath components [1–6]. Therefore, TOA of the received signal can be estimated with high accuracy for 60 GHz systems if the first arriving path has been identified precisely. One of major challenges for localization systems is mitigation of NLOS effects. If direct path between a fixed terminal (FT) (An FT is usually a base station in a cellular network or an anchor node in a sensor network.) and MT is being obstructed, TOA of signal to FT will be delayed, which introduces a positive bias. Using such NLOS TOA estimates during localization of MT position may significantly degrade positioning accuracy. Hence, FTs that are under NLOS condition have to be identified and their effects have to be mitigated.

NLOS identification and mitigation techniques have been discussed extensively in the literature, but mainly within cellular network framework [7–13]. For example, in [7], skewness of ranging measurements is compared with threshold for NLOS identification, where measurement noise variance is assumed to be known. In [8], a decision-theoretic NLOS identification framework is presented, where various hypothesis tests are discussed for known and unknown probability density functions (PDFs) of TOA measurements. Guvenc *et.al*. [9-13] used mean excess delay, root mean square (RMS) delay, and kurtosis of multipath channel as NLOS identification metrics. When statistics of kurtosis, mean

ISSN: 1975-4094 IJSH

excess, and RMS delays are priori known, likelihood ratio tests can be performed for hypothesis selection. Another method was proposed by Heidari *et.al*. [10]. They tried to find the first detected path of the received signal as a peak of filtered channel impulse radio. As similar to previous method, this technique also used joint likelihood function using mean excess delay τ_{med}, total received power P_{tot} and hybrid of power of the first detected path and TOA of the first detected path ξ_{hyb} .Venkatesh *et.al*. [11] identified channel based on TOA, RSS, and RMS delay spread (RDS) of the received signal. The conditional distributions of TOA, RSS, and RDS estimates are functions of distance and channel state. Provided that the physical distance between the transmitted and receive nodes is known exactly, state of channel can be identified by comparing likelihood values for each of estimates (TOA, RSS, and RDS), conditioned on distance. Shimizu *et.al*. [12] performed intensive measurements of path-loss and delay-profile characteristics of LOS and NLOS environments in a suburban residential area. Based on their analysis, they found that delay spread was dependent on distance, and NLOS delay spread was found to be several times larger than that of LOS case. The skewness of delay spread for NLOS cases ranged from 80 to 200 ns, which was an order of magnitude larger than that of LOS case.

In this paper, we propose a new LOS/NLOS identification approach for 60 GHz signal, which is based on maximum slope and kurtosis of energy block of the received signal using energy detector (ED). Firstly, we use ED TOA estimation algorithm for estimation TOA. Secondly, we characterize maximum slope and kurtosis of energy block of the received signal. Finally, we use a threshold test for LOS/NLOS identification.

The remainder of this paper is organized as follows. Section 2 describes the signal and channel model. Section 3 describes LOS/NLOS identification approach and presents results of the numerical simulations. The concluding remarks are given in Section 4.

2. System Model

Currently, there are two important standards that have been developed for 60 GHz wireless communications systems, IEEE 802.15.3c and IEEE 802.11ad [14-15]. In this paper, the channel models in IEEE 802.15. 3c standard are used because it is specifically designed for wireless personal area networks and thus encompasses typical indoor environments. Further, these are the most widely employed models for 60 GHz systems. IEEE 802.15.3c standard was the first developed for high data rate short-range wireless systems. The physical layer was designed to support the transmission of data within a few meters at a maximum data rate of 2 Gbps. These models have been developed for communications in frequency band 57 to 66 GHz in indoor residential, indoor office and library environments (with differences largely due to the LOS and NLOS characteristics) [16-20]. In this paper, a pulse position modulation time hopping 60 GHz signal is employed for ranging purposes. The propagation delay $\hat{\tau}$, between transmitter and receiver is estimated for use in localization.

2.1. 60GHz Signal

The 60 GHz signals have a very short duration (typically 100 picoseconds or less), and can be expressed as:

$$s(t) = \sum_{-\infty}^{\infty} p\left(t - jT_s - C_j T_c - a_j \varepsilon\right) \tag{1}$$

where T_s is symbol time. The Time Hopping (TH) code represented by C is a pseudorandom integer-valued sequence which is unique for each user to limit multiple access interference, and T_c is chip time. PPM time shift is ε so that if a_j is 1, the signal is shifted in time by ε , while if a_j is 0, there is no shift. Many pulse shapes have been proposed for 60 GHz systems. In this paper a Gaussian pulse is employed which is multiplied by the carrier signal to give:

$$p(t) = \frac{\sqrt{2}}{\alpha} \exp\left(-2\pi \frac{t^2}{\alpha^2}\right) \cos(2\pi f_c t) \tag{2}$$

where α is shape factor and f_c is carrier frequency which here is $f_c = 60$ GHz. A smaller shape factor results in a shorter duration pulse and a larger bandwidth.

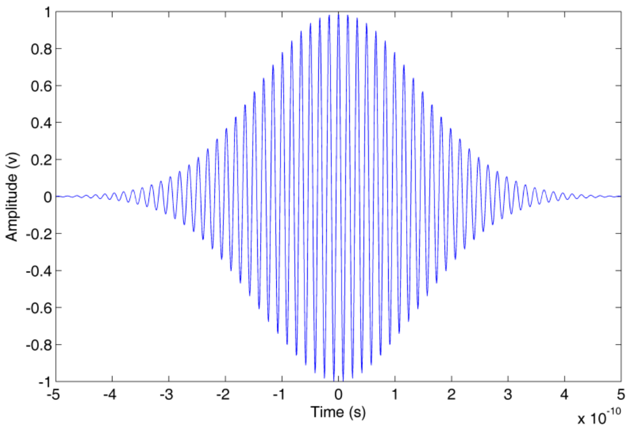

Figure 1. Waveform of 60 GHz Signal

2.2. Signal Shift and Path Loss

The path loss is defined as ratio of the received signal power to transmit signal power and it is very important for link budget analysis. Unlike narrow-band system, path loss for a wide-band system such as mm-wave system, is both distance and frequency dependent. In order to simplify the models, it is assumed that frequency dependence path loss is negligible and only distance dependence path loss is modeled. The signal path loss, which depends on propagation distance and channel (IEEE802.15.3c), is described by:

$$PL(d)[dB] = PL_0 + 10 \cdot n \log_{10}\left(\frac{d}{d_0}\right) + X_\sigma [dB]; \quad d \geq d_0 \tag{3}$$

where d_0 and d denote reference distance, and distance respectively. n is path loss exponent for mm-wave. X_σ is that the unit *dB*, with mean zero and variance σ_s for a Gaussian random variable. Table 1 summarizes the values of n, PL_0, σ_s for different environments and scenarios.

Table 1. Values of n, PL_0, σ_s for Different Environments and Scenarios

environments	n	PL_0	σ_s
indoor residential (LOS)	1.53	75.1	1.50
indoor residential (NLOS)	2.44	86.0	6.20
indoor office (LOS)	1.16	84.6	5.40
indoor office (NLOS)	3.74	56.1	8.60

The signal shift can be expressed as:

$$t = dt * floor((d / c)/dt) \tag{4}$$

where d denotes the distance between the transmitter and receiver, dt is the sampling period and c is the speed of light which is 299792458m/s in the air.

2.3. Multipath Fading Channel

The received signal can be written as:

$$r(t) = \sum_{n=1}^{N} \alpha_n p(t - \tau_n) + n(t) \tag{5}$$

where N is number of received multipath components, α_n and τ_n denotes amplitude and delay of the nth path respectively, $p(t)$ is the received 60 GHz pulse and $n(t)$ is additive white gaussian noise with zero mean and two sided power spectral density $N_0/2$. Equation (5) can be rewritten as:

$$r(t) = s(t) * h(t) + n(t) \tag{6}$$

where $s(t)$ is transmitted signal, and $h(t)$ is channel impulse response which can be expressed as:

$$h(t,\theta) = \sum_{k=1}^{K} \sum_{l=1}^{L_k} \mu_{kl} \delta(t - T_k - \tau_{kl}) \delta(\theta - \theta_k - \omega_{kl}) \tag{7}$$

where $\delta(.)$ is Dirac-delta function, K is number of clusters, L_k is number of rays in the k^{th} cluster, and μ_{kl}, τ_{kl} and ω_{kl} denote complex amplitude, delay and azimuth of the k^{th} ray of the l^{th} cluster, respectively. Similarly, T_k and θ_k represent delay and mean AOA of the k^{th} cluster.

2.4. Energy Detector

After the amplifier, the received signals are squared, and then input to an integrator with integration period Tb. Because of inter-frame leakage due to multipath signals, integration duration is $3T_f/2$, so number of signal values for ED is $N = 3T_f/2Tb$. The integrator outputs can be expressed as:

$$z[n] = \sum_{i=1}^{N} \int_{(i-1)T_f + (c_j + n - 1)Tb}^{(i-1)T_f + (c_j + n)Tb} r^2(t) dt \tag{8}$$

Where $n \in \{1, 2, .., N\}$ denotes the sample index with respect to the starting point of the integration period and N is the number of pulses per symbol. Here, N is set to 1, so the integrator outputs are

$$z[n] = \sum_{i=1}^{N} \int_{(c_j + n - 1)Tb}^{(c_j + n)Tb} r^2(t) dt \tag{9}$$

If $z[n]$ is integration of noise only, it has a centralized Chi-square distribution, while it has a non-centralized Chi-square distribution if a signal is present. The mean and variance of the noise and signal values are given by [17] respectively.

$$\mu_0 = F\sigma^2, \sigma_0 = 2F\sigma^4 \tag{10}$$

$$\mu_e = F\sigma^2 + E_n, \sigma_e^2 = 2F\sigma^4 + 4\sigma^2 E_n \tag{11}$$

where E_n is signal energy within the n^{th} integration period and F is number of degrees of freedom given by $F = 2BTb + 1$. Here B is signal bandwidth.

3. LOS/NLOS Identification

3.1. Description of Parameters

In this paper, we distinguish between LOS or NLOS scenarios by exploiting statistics of the received signal by ED. Maximum slope and kurtosis of energy block is used in order to identify LOS and NLOS scenarios respectively. Slope of energy values is considered as a measure. These values are divided into (N-M+1) groups, with *M* values in each group. The slope for each group is calculated using a least squares line-fit. The maximum slope can then be expressed as:

$$MS = \max_{1 \le n \le N-M+1} slope\left\{ linefit\left(z[n], z[n+1], \ldots.., z[n+M-1] \right) \right\} \quad (12)$$

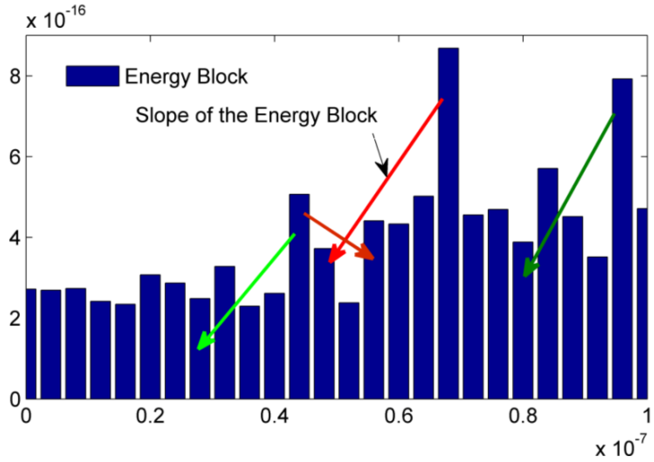

Figure 2. Slope of Energy Block

Kurtosis is calculated using the second and fourth order moments and is given by:

$$K = \frac{E\left[(x_i - \mu_x)^4 \right]}{E\left[(x_i - \mu_x)^2 \right]^2} = \frac{E\left[(x_i - \mu_x)^4 \right]}{\sigma_x^4} \quad (13)$$

where μ_x is mean value and σ_x is standard deviation. Kurtosis for a standard normal distribution is three. For this reason, kurtosis is often redefined as $K = K - 3$ (often referred to as "excess kurtosis"), so that standard normal distribution has a kurtosis of zero, positive kurtosis indicates a "peaked" distribution and negative kurtosis indicates a "flat" distribution. For noise only (or for a low SNR) and sufficiently large *F* (degrees of freedom of the Chi-square distribution), $z[n]$ has a Gaussian distribution and kurtosis=0. On the other hand, as SNR increases, kurtosis will tend to increase.

3.2. Identification Approach

The ratio values of slope and kurtosis of energy block can be obtained for both LOS and NLOS scenarios using sample channel realizations from both scenarios. Here, we used sample channel realizations of IEEE 802.15.3c standard channel models in order to obtain the values of slope and kurtosis of energy slope for both LOS and NLOS. In order to examine the characteristics of ratio of kurtosis and maximum slope, CM1.1 (residential LOS) and CM2.1 (residential NLOS) channel models from IEEE 802.15.3c standard are employed. For each SNR value, 1000 channel realizations are generated and sampled at $f_c = 1 \cdot e^{10}$ Hz. The other system parameters are $T_f = 200ns, T_c = 1ns$, Tb is from 1 ns to 4 ns and *N* = 1. Each realization has a TOA uniformly distributed within $(0 - T_f)$. Here SNR ranges from 0dB to 7dB, 1000 channel realizations are generated for each SNR. CM1.1 and CM2.1 from IEEE 802.15.3c standard are employed. Here are 8*1000 samples which are got for each channel model. The relationship between ratio values and SNR are shown in Figures 3-6.

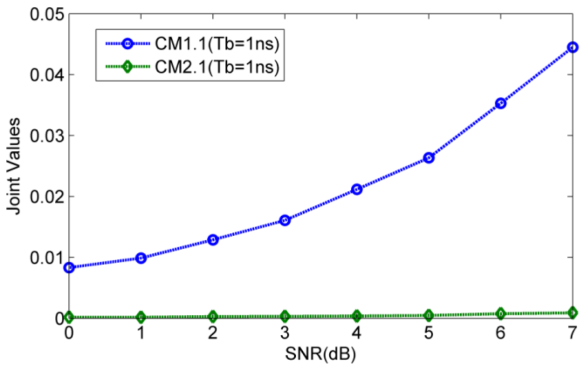

Figure 3. Joint Values with Respect to SNR (CM1.1 and CM2.1 with Tb=1ns)

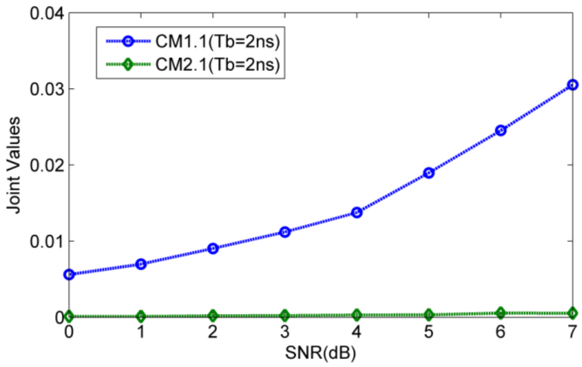

Figure 4. Joint Values with Respect to SNR (CM1.1 and CM2.1 with Tb=2ns)

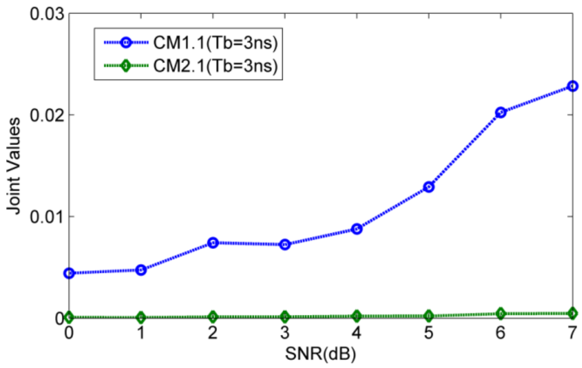

Figure 5. Joint Values with Respect to SNR (CM1.1 and CM2.1 with Tb=3ns)

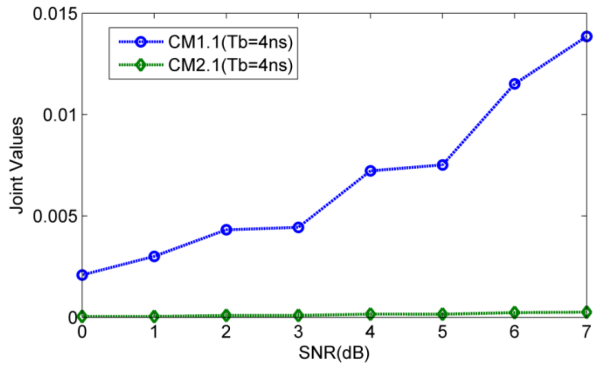

Figure 6. Joint Values with Respect to SNR (CM1.1 and CM2.1 with Tb=4ns)

From Figures 3-6, results show that ratio values are monotonous with respect to SNR (both LOS and NLOS environment) in 60 GHz wireless communication system respectively. But we find maximum of joint values (LOS) is even less than maximum of joint values (NLOS) when *TX* is 360^{o}, maximum of joint values (LOS) is even larger than maximum of joint values (NLOS) when *TX* is others. So we propose a novel method to identify the LOS and NLOS which can be expressed as:

$$\Theta = \alpha \begin{cases} \begin{cases} < \alpha_{MS} \Rightarrow NLOS \\ > \alpha_{MS} \Rightarrow LOS \end{cases} & TX = 360^{\circ} \\ \begin{cases} < \alpha_{MS} \Rightarrow LOS \\ > \alpha_{MS} \Rightarrow NLOS \end{cases} & TX < 360^{\circ} \end{cases} \tag{14}$$

Where α_{MS} is threshold which is chosen to identify LOS and NLOS, *TX*, *RX* is beam-width of measured transmitter and receiver antenna respectively. Aiming at ranges [A, B] dB for SNR, α_{MS} can be shown as follows :

$$\alpha_{MS} = \min \begin{Bmatrix} mean\left[find\left(P\left(abs(MS) < \Theta_1 |_A \right) \geq \Phi \right) \right] \\ mean\left[find\left(P\left(abs(MS) < \Theta_2 |_B \right) \geq \Phi \right) \right] \end{Bmatrix} \tag{15}$$

Where Θ_1 and Θ_2 are threshold which meet the condition $P(MS > \Theta) \geq \Phi$ where SNR is upper and lower limits. Φ is probability value which is required for choosing suitable threshold for NLOS identification. As shown in Figure 7, the distribution of *K/M* samples larger than a certain threshold value Θ for IEEE802.15.3c channel. When Θ is set to be 0.1 and more than 950 of the 1000 *K/M* samples are distributed less than Θ . In the process of simulation, results show that if we use those samples whose probability distribution is high, we can guarantee accuracy of NLOS identification and remove some extreme values at the same time. Without loss of generality, here Φ is set to be 0.85.

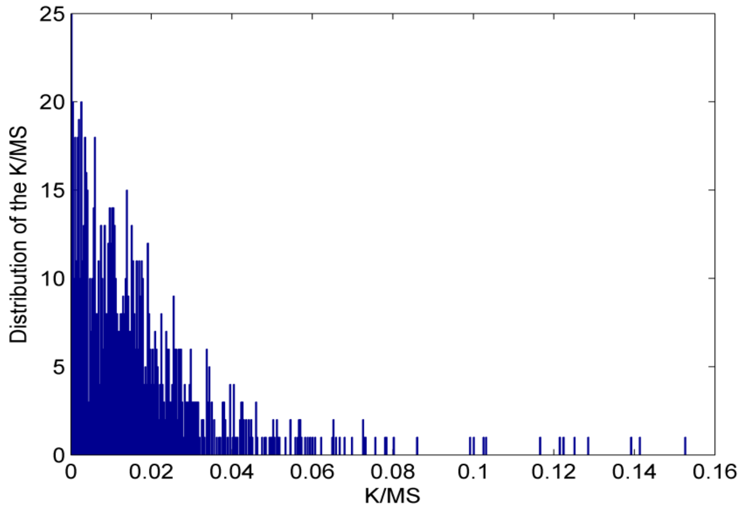

Figure 7. Distribution of K/M

In order to verify the effectiveness and practicality of the algorithm, so we make a lot of simulations using IEEE 802.15.3c channel models. CM1.2, CM1.3, CM1.4 (residential LOS) and CM2.2, CM2.3, CM2.4 (residential NLOS) channel models from IEEE 802.15.3c standard are employed. For each SNR value, 1000 channel realizations are generated and sampled at $f_c = 1 \cdot e^{10}$ Hz. The other system parameters are $T_f = 200ns$, $T_c = 1ns$, $Tb = 1ns \; and \; 4ns$ and N = 1. Each realization has a TOA uniformly distributed within $(0 - T_f)$. Here SNR ranges from 0 dB to 7 dB, 1000 channel realizations are generated for each SNR. CM1.2, CM1.3, CM1.4 (residential LOS) and CM2.2, CM2.3, CM2.4 (residential NLOS) channel models from IEEE802.15.3c standard are employed. Here are 8*1000 samples which are got for each channel model. The relationship between joint parameter and SNR are shown in Figures 8-19.

In order to verify effectiveness of NLOS identification algorithm, 1000 channel realizations were generated when SNR is from 0 dB to 7 dB in each IEEE802.15.3c channel and other system parameters as above. The threshold values and accuracy for identifying LOS and NLOS were calculated for each IEEE802.15.3c channel model. As shown in Table 2, accuracy increases for LOS environment and decreases for NLOS environment as the SNR increases when $TX = 360$. Conversely, accuracy increases for NLOS environment and decreases for LOS environment as the SNR increases when $TX < 360$. Accuracy of LOS/NLOS identification is higher than any other identification algorithms based on energy detect such as in [21], the accuracy is only around 60% while the accuracy of the proposed algorithm over 70% for most channel model.

Table 2. Threshold Values for LOS and NLOS Identification

Channel Model	1 (dB)	2 (dB)	3 (dB)	4 (dB)	5 (dB)	6 (dB)	Mean Values	Threshold Values
CM1.1	62.5	67.2	73.1	76.9	84.0	85.4	74.85	0.0115
CM2.1	68.2	64.8	61.2	57.7	51.6	47.8	58.55	
CM1.2	95.0	90.3	85.0	74.8	66.3	55.8	77.86	0.0695
CM2.2	81.9	85.3	86.8	90.9	91.1	92.9	88.15	
CM1.3	93.1	90.4	86.2	77.8	66.1	57.7	78.55	0.0715
CM2.3	95.6	97.5	96.9	98.2	98.1	99.2	97.58	
CM1.4	94.5	91.9	86.6	78.6	70.5	58.4	80.08	0.0775
CM2.4	94.7	96.7	95.6	96.9	97.8	98.7	96.73	

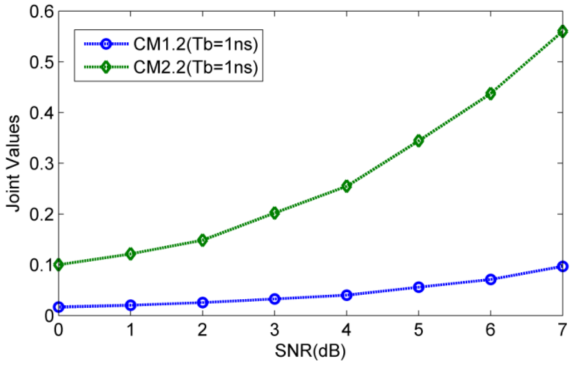

Figure 8. Joint Values with Respect to SNR (CM1.2 and CM2.2 with Tb=1ns)

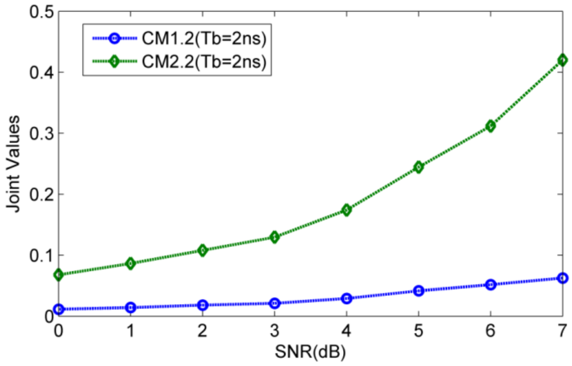

Figure 9. Joint Values with Respect to SNR (CM1.2 and CM2.2 with Tb=2ns)

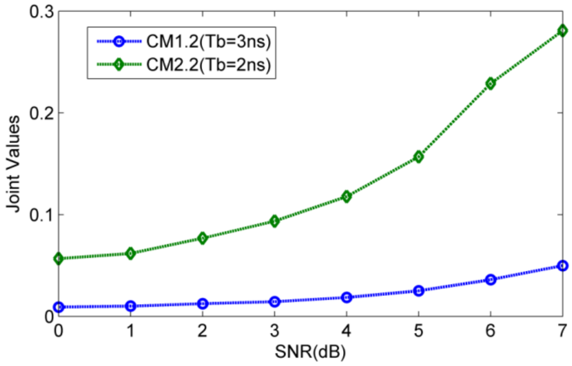

Figure 10. Joint Values with Respect to SNR (CM1.2 and CM2.2 with Tb=3ns)

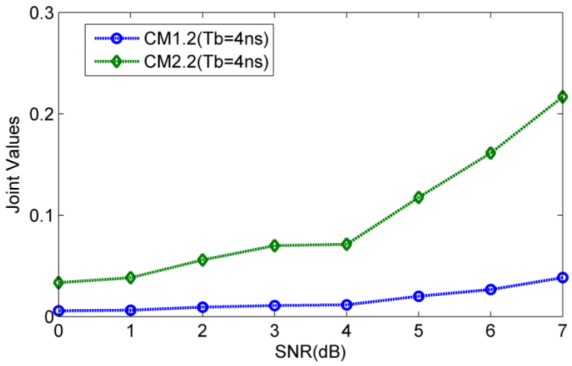

Figure 11. Joint Values with Respect to SNR (CM1.2 and CM2.2 with Tb=4ns)

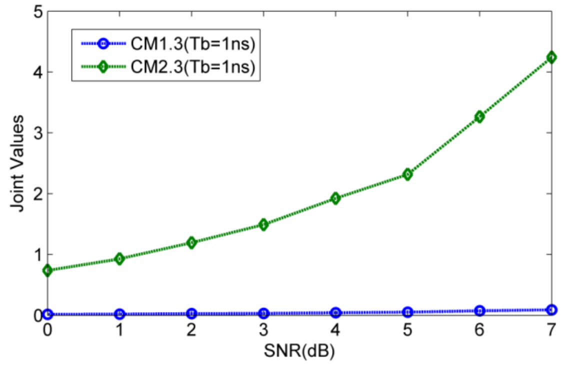

Figure 12. Joint Values with Respect to SNR (CM1.3 and CM2.3 with Tb=1ns)

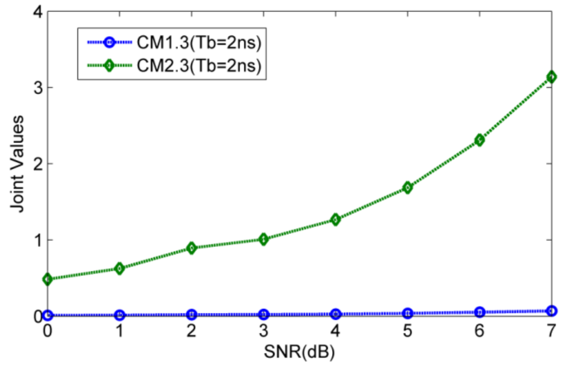

Figure 13. Joint Values with Respect to SNR (CM1.3 and CM2.3 with Tb=2ns)

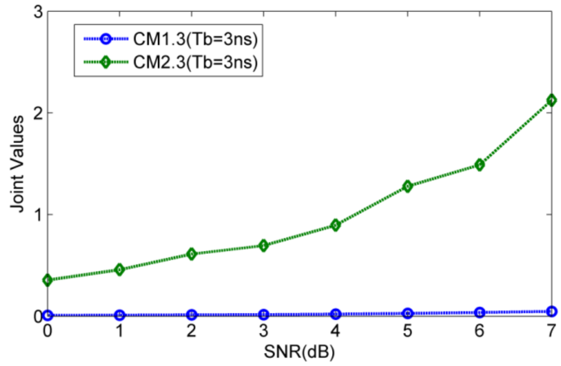

Figure 14. Joint Values with Respect to SNR (CM1.3 and CM2.3 with Tb=3ns)

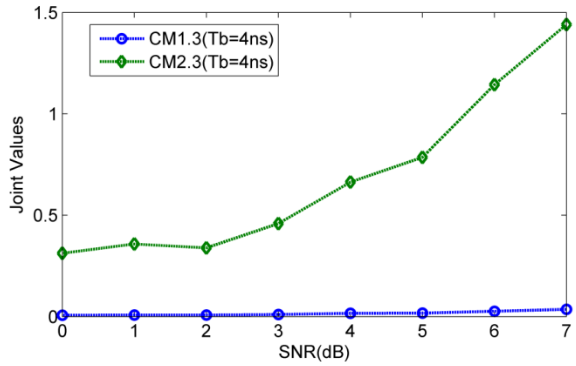

Figure 15. Joint Values with Respect to SNR (CM1.3 and CM2.3 with Tb=4ns)

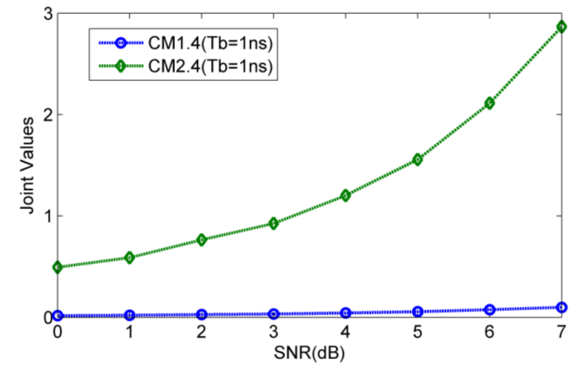

Figure 16. Joint Values with Respect to SNR (CM1.4 and CM2.4 with Tb=1ns)

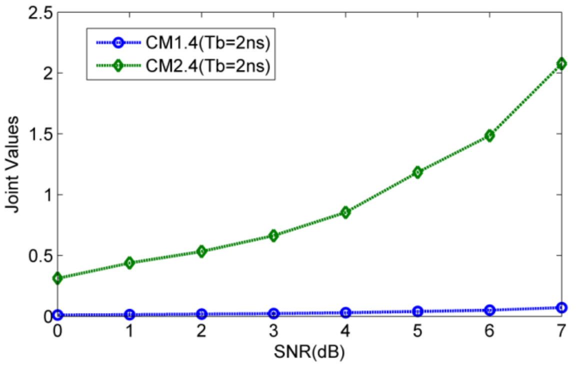

Figure 17. Joint Values with Respect to SNR (CM1.4 and CM2.4 with Tb=2ns)

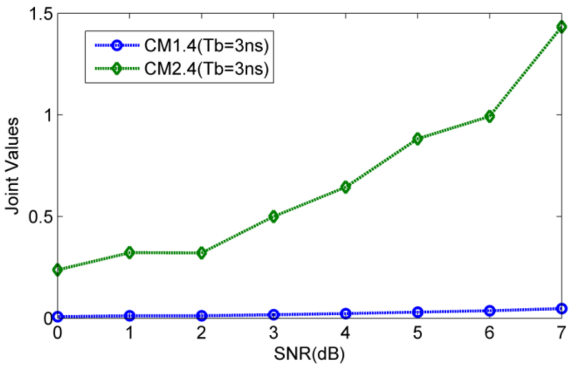

Figure 18. Joint Values with Respect to SNR (CM1.4 and CM2.4 with Tb=3ns)

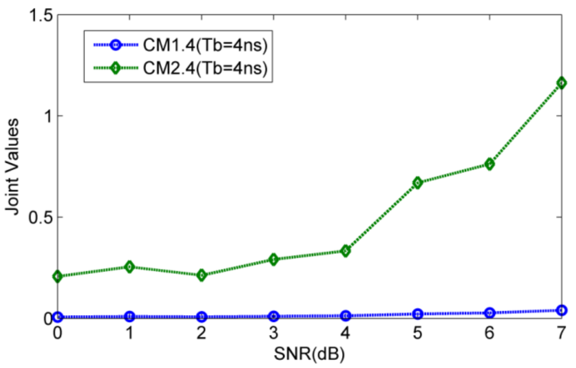

Figure 19. Joint Values with Respect to SNR (CM1.4 and CM2.4 with Tb=4ns)

4. Conclusion

In this paper, we presented a novel approach to deal with NLOS propagation that relies solely on features extracted from the received waveform. This technique does not require formulation of explicit statistical models for features which is based on maximum slope and kurtosis of energy block of the received signal using ED. In order to verify effectiveness and practicality of algorithm, so we make a lot of simulations using IEEE 802.15.3c channel models. CM1.1, CM1.2, CM1.3, CM1.4 (residential LOS) and CM2.1, CM2.2, CM2.3, CM2.4 (residential NLOS) channel models from IEEE 802.15.3c standard are employed. Results show that joint parameter can identify LOS and NLOS environments so long as the threshold α_{MS} can be fixed bitterly. We developed techniques that are capable of distinguishing LOS/NLOS propagation in NLOS conditions. Our results revealed that the proposed technique outperforms previous parametric techniques from the literature. But here is a question that the method we proposed can't identify the LOS and NLOS environments in the office. So in the future, this will be the problem which is eager to be solved for us.

Acknowledgments

The authors would like to thank colleagues from UWB Laboratory in College of Information Science and Engineering, Ocean University of China, for help with obtaining the measurement data. This work was supported by Nature Science Foundation of China under Grant No. 60902005, Qingdao International Science and Technology Cooperation Projects of Qingdao under Grant No. 12-1-4-137-hz, Nature Science Foundation of China under Grant No. 61301139, Nature Science Foundation of Shandong Province No. ZR2014FL014, Science and Technology Project in Colleges and Universities of Shandong Province No.J14LN53, Project of Basic Research Application of Qingdao City No. 14-2-4-37-jch and Project of Basic Research Application of Qingdao City No. 14-2-4-83-jch.

Reference

[1] L. Zhang, "A fully integrated 60GHz four channel CMOS receiver with 7GHz ultra-wide band width for IEEE 802.11ad standard", Communication, China, vol. 11, no. 6, **(2014)**, pp. 42-50.

[2] S. K. Yong and C. C. Chong, "An overview of multi gigabit wireless through millimeter Wave Strategy: Potentials and Technical Challenges", EURASIP J. Wireless Communications and Networking, vol. 2007, no. 1, **(2007)**, pp. 1-10.

[3] R. C. Daniels and R. W. Heath, "60 GHz wireless communications: emerging requirements and design recommendations", IEEE Vehicular Strategy Society, vol. 2, **(2007)**, pp. 41-50.

[4] C. C. Chong, F. M. Peter, Smulders, "60GHz-Millimeter-Wave Radio Principle, Strategy, and News Results", EURASIP Journal on Wireless Communications and Networking, vol. 2007, no. 1, **(2007)**, pp. 1-8.

[5] S. K. Yong, P. F. Xia and V. G. Alberto, "60-GHz Strategy for Gbps WLAN and WPAN: From Theory to Practice", Beijing: Press of China Machine, **(2013)**.

[6] R. C. Daniels and R. W. Health, "60 GHz wireless communications: emerging requirements and design recommendations", IEEE Vehicular Strategy Magazine, vol. 2, no. 3, **(2007)**, pp. 41-50.

[7] M. P. Wylie and J. Holtzman, "The non-line of sight problem in mobile location estimation", Proceedings of the 5th IEEE International Conference on Universal Personal Communications (ICUPC '96), Cambridge, Mass,USA, vol. 2, **(1996)** September-October, pp. 827-831.

[8] J. Borras, P. Hatrack and N. B. Mandayam, "Decision theoretic framework for NLOS identification", Proceedings of the 48th IEEE Vehicular Technology Conference (VTC '98), Ottawa, Canada, vol. 2, **(1998)** May, pp. 1583-1587.

[9] I. Guvenc, C-C Chong and F. Watanabe, "NLOS identification and mitigation for UWB localization systems. Wireless Communications and Networking Conference", WCNC 2007. IEEE, **(2007)**, pp. 1571-1576.

[10] M. Heidari, F. O. Akgul and K. Pahlavan, "Identification of the absence of direct path in indoor localization systems", IEEE International Symposium on Personal, Indoor, and Mobile Radio Communications, **(2007)**, pp. 1-6.

[11] S. Venkatesh and R. M. Buehrer, "Non-line-of-sight identification in ultra-wideband systems based on received signal statistic", Microwaves, Antennas & Propagation, IET, vol. 1, no. 6, **(2007)**, pp. 1120-1130.

[12] H. Shimizu, H. Masui, M. Ishii and K. Sakawa, "LOS and NLOS path-loss and delay characteristics at 3.35 GHz in a residential environment", Antennas and Propagation Society International Symposium, IEEE, vol. 2, **(2000)**, pp. 1142-1145.

[13] I. Güvenç I, C-C Chong, F. Watanabe and H. Inamura, "NLOS identification and weighted least-squares localization for UWB systems using multipath channel statistics", EURASIP Journal on Advances in Signal Processing, 2008:14 Article ID 271984, **(2008)**.

[14] "IEEE Standard for Information strategy--Local and metropolitan area networks--Specific requirements--Part 15.3: Wireless Medium Access Control (MAC) and Physical Layer (PHY) Specifications for High Rate Wireless Personal Area Networks (WPAN) amendment 2: millimeter-wave-based alternative physical layer extension". IEEE Computer Society, IEEE 802.15.06-0474-00-003c. New York, USA, **(2009)**.

[15] "802.11n-2009-IEEE Standard for Information strategy-- Local and metropolitan area networks--Specific requirements--Part 11: Wireless LAN Medium Access Control (MAC)and Physical Layer (PHY) Specifications Amendment 5: Enhancements for Higher Throughput", IEEE Computer Society, IEEE 978-0-7381-6731-2. New York, USA, **(2009)**.

[16] C. R. Andersonn and T. S. Rappaport, "In-building wideband partition loss measurements at 2.5 and 60GHz", IEEE Transactions on Wireless Communications, vol. 3, no. 3, **(2004)**, pp. 922-928.

[17] S. Collong, G. Zaharia and G. E. Zein, "Influence of the human activity on wide-band characteristics of the 60GHz indoor radio channel", IEEE Transactions on Wireless Communications, vol. 3, no. 6, **(2005)**, pp. 2396-2406.

[18] A. Maltsev, R. Maslennikov and A. Sevastyanov, "Experimental investigations of 60GHz WLAN systems in office environment", IEEE Journal on Selected Areas in Communications, vol. 27, no. 8, **(2009)**, pp. 1488-1499.

[19] M. G. Sanchez, A. V. Alejos and I. Cuinas, "Comparision of space diversity performance in indoor radio channels at 40GHz and 60GHz", Proc. of European Conference on Wireless Strategy, Amsterdam, **(2008)**.

[20] H. B. Yang, "Channel characteristics and transmission performance for various channel configurations at 60GHz", EURASIP Journal on Wireless Communications and Networking, vol. 2007, no. 1, **(2007)**, pp. 43-43.

[21] S. H. WU, Q. Y. Zhang and N. T. Zhang, "NLOS Identification for IR-UWB Ranging Systems", Journal of Electronics & Information Technology ,vol. 30, no. 11, **(2008)**, pp. 2541-2546.

Authors

Xiao-Lin Liang, now studies in College of Information Science and Engineering and is a Ph. D. candidate in Ocean University of China. His research interests include ultra-wideband radio systems, 60GHz wireless communication system.

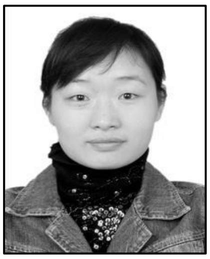

Ting-Ting Lu, received the Ph. D. degree in College of Information Science and Engineering from Ocean University of China in 2013. She is now a lecture in College of Information Science and Engineering. Her research interests include ultra-wideband radio systems, 60GHz wireless communication system.

Hao Zhang, received the MBA degree in New York Institute of Technology, American in 2001 and the Ph. D. degree in Electrical and Computer Engineering from the University of Victoria, Canada in 2004. He was a Project Manager for Microsoft Inc. in United States during January 2000-May 2000. During 2004-2008, he was the Vice President for the United States Gamma Capital Inc. He is now an Adjunct Assistant Professor in the Department of Electrical and Computer Engineering. Also he becomes a professor and the Ph. D. supervisor in College of Information Science and Engineering from Ocean University of China in 2006. His research concerns ultra-wideband radio systems, 60GHz wireless communication system and MIMO wireless communication.

T. Aaron. Gulliver received the Ph. D. degree in Electrical and Computer Engineering from the University of Victoria, Canada in 1989. He is now a professor and the Ph. D. supervisor in the Department of Electrical and Computer Engineering. In 2002, he becomes a Fellow of the Engineering Institute of Canada, and in 2012 a Fellow of the Canadian Academy of Engineering. He is also a senior member of IEEE. His research concerns information theory and communication theory, algebraic coding theory and smart grid and ultra-wideband communication.

